ITCH

# Inhibition of natriuretic peptide receptor 1 reduces itch in mice

**Hans Jürgen Solinski[1], Patricia Dranchak[2], Erin Oliphant[2], Xinglong Gu[1], Thomas W. Earnest[1], John Braisted[2], James Inglese[2], Mark A. Hoon[1]***



**There is a major clinical need for new therapies for the treatment of chronic itch. Many of the molecular components involved in itch neurotransmission are known, including the neuropeptide NPPB, a transmitter required for normal itch responses to multiple pruritogens in mice. Here, we investigated the potential for a novel strategy for the treatment of itch that involves the inhibition of the NPPB receptor NPR1 (natriuretic peptide receptor 1). Because there are no available effective human NPR1 (hNPR1) antagonists, we performed a high-throughput cell-based screen and identified 15 small-molecule hNPR1 inhibitors. Using in vitro assays, we demonstrated that these compounds specifically inhibit hNPR1 and murine NPR1 (mNPR1). In vivo, NPR1 antagonism attenuated behavioral responses to both acute itch– and chronic itch–challenged mice. Together, our results suggest that inhibiting NPR1 might be an effective strategy for treating acute and chronic itch.**

## INTRODUCTION

Itch is an unpleasant sensation associated with skin irritation that elicits the strong urge to scratch. Whereas most itch has a relatively low prevalence and is easily managed (*1*), chronic itch has a major negative impact on quality of life, and current treatments are largely ineffective (*2*, *3*). The underlying pathophysiological mechanisms for chronic itch are poorly understood (*4*, *5*). For this reason, clinically chronic itch is categorized on the basis of its apparent origin with dermatological, systemic, neurological, somatoform, and mixed pruritus (*6*). Itch stimuli themselves are thought to be detected in the skin by dedicated sensory neurons that innervate the skin and express G protein–coupled, Toll-like, and interleukin receptors (*5*, *7*–*11*). Whereas the repertoire of known receptors is large, the number of itch cell types that detect itch stimuli is small. The itch-sensory neurons comprise two distinct populations: those expressing the mas-related G protein–coupled receptor A3 (*Mrgpra3*) and those expressing the neuropeptide natriuretic polypeptide b (*Nppb*) (*12*, *13*). Both these classes of neurons transmit itch through a common spinal cord circuit dependent on NPPB (*14*, *15*). In addition, sensory neuron–derived NPPB has recently been suggested to drive inflammation in different forms of dermatitis, in both humans and mice, thereby enhancing pruritus (*16*).

Work from our laboratory identified the spinal cord receptor for NPPB, natriuretic peptide receptor 1 (NPR1), as a potential target for the treatment of itch (*13*). We demonstrated that elimination of NPPB as well as the ablation of spinal interneurons expressing *Npr1* profoundly attenuated scratching responses to many pruritogens in mice (*13*). These results indicate that NPPB is a critical component required for the excitation of spinal cord *Npr1*-expressing interneurons. The NPR1 receptor belongs to a small guanylate cyclase (GC) family of receptor proteins that are specifically activated by natriuretic peptides (NPs) (*17*). NPR1 binds both NPPB and NPPA with high affinity and has a much lower affinity for the third NP, NPPC (*17*). Three cyclic peptide analogs of NPPB have been reported to inhibit NPR1 (*18*–*21*). However, one of these, A-71915, was reported to be ineffective at blocking itch in mice. Specifically, A-71915, when administered intrathecally, was unable to attenuate acute itch (*22*). This result suggests that inhibition of spinal cord NPR1 may not be an effective method for relieving itch. To investigate this further, we characterized the properties of A-71915 and found that the compound is a strong partial agonist, not a neutral antagonist, of murine NPR1 (mNPR1), suggesting a possible explanation for its lack of potency in relieving itch. Using high-throughput screening (HTS), we identified human NPR1 (hNPR1) antagonists and show that one of these compounds can relieve itch in vivo in mouse models of itch.

## RESULTS

### Similar expression of *NPPB* in human and mouse dorsal root ganglia neurons

Research on the basic mechanism for itch has been predominantly performed in the mouse animal model (*4*). The molecules for many pathways in sensory neurons in humans and mice have been assumed to be similar to each other, although in some instances the molecules may not be the same (*23*–*25*). Therefore, as a starting point, to motivate the investigation of NPPB as a target for development of itch therapies, we examined whether human dorsal root ganglia (DRG) express *NPPB*. We detected, by quantitative polymerase chain reaction (qPCR), similar amounts of *NPPB* transcripts in complementary DNA (cDNA) from human and mouse DRG (Fig. 1A). In concordance with this result, using double-label in situ hybridization (ISH), we found that the numbers of NPPB neurons (9.8 ± 1.9%; 200 of 2086 neurons, $n = 4$ donors) in human DRG are approximately the same as previously reported in mice (*26*), and human NPPB neurons likewise have small to medium diameter (Fig. 1, B and C). In mice, *Nppb* is coexpressed with *TrpV1* (*13*). Therefore, if NPPB has a comparable role in humans, then it should have a similar distribution in human DRG. ISH revealed, similar to mouse (*26*), that all *NPPB*-positive human DRG neurons coexpress *TRPV1* (150 neurons, $n = 4$ donors) and that these neurons are a fraction of the *TRPV1* neurons (Fig. 1, D and E). In addition, for NPPB to function in a similar way in humans to that reported in mice (*13*), its receptor

[1]Molecular Genetics Section, National Institute of Dental and Craniofacial Research/NIH, 35 Convent Drive, Bethesda, MD 20892, USA. [2]Division of Pre-Clinical Investigation, National Center for Advancing Translational Sciences, National Institutes of Health, Rockville, MD 20850, USA.
*Corresponding author. Email: mark.hoon@nih.gov

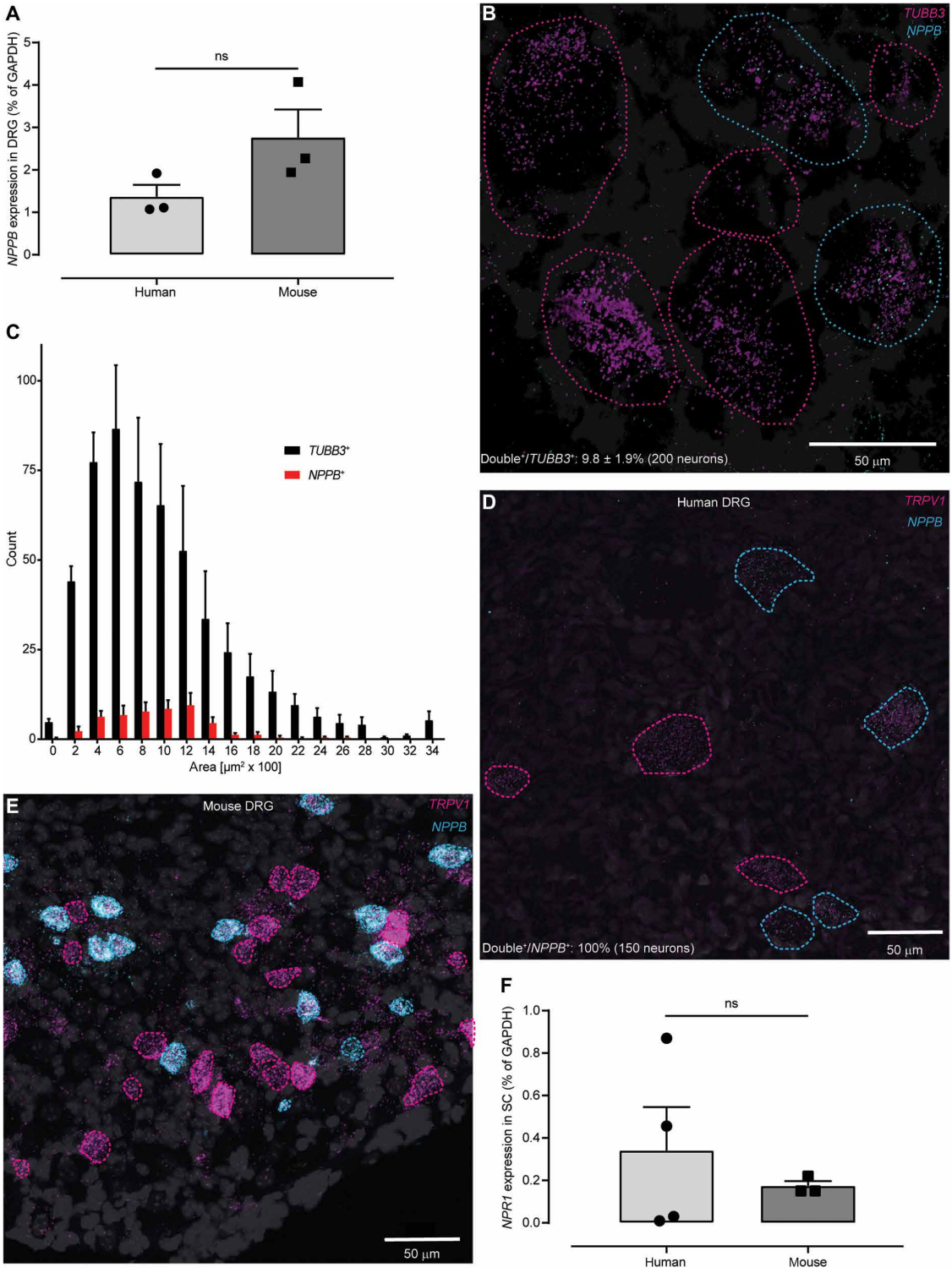


**Fig. 1. The NPPB-NPR1 itch signaling pathway is conserved between mice and humans.** (**A**) qPCR-based quantification of expression did not show a significant difference in amounts of *NPPB* transcripts between human and mouse DRG ($P = 0.1241$, unpaired $t$ test; $n = 3$). (**B**) Representative double ISH images of a field of human DRG with neurons stained for *NPPB* (cyan) and *TUBB3* (magenta). *NPPB*-positive and *NPPB*-negative neurons are outlined with cyan and magenta dots, respectively. DAPI (4′,6-diamidino-2-phenylindole) counterstain is displayed in gray. (**C**) Quantification of the soma size of *NPPB*-stained (red) compared to *TUBB3*-stained (black) neurons ($n = 4$). Representative double ISH images of fields of human (**D**) and mouse (**E**) DRG reveal that *NPPB* (cyan) and *TRPV1* (magenta) are coexpressed. In human and mouse DRG, *NPPB* is expressed in a subset of *TRPV1* neurons (cyan dotted profiles) and single-labeled *TRPV1* neurons are indicated with magenta dotted profiles. (**F**) qPCR-based quantification of expression did not show a significant difference in amounts of *NPR1* transcripts between human and mouse spinal cord (SC) [not significant (ns), $P > 0.9999$, Mann-Whitney; $n = 4$ (human) and 3 (mouse)]. GAPDH, glyceraldehyde-3-phosphate dehydrogenase.

*NPR1* should be expressed in spinal cord. To test this, we compared expression of human and mouse *Npr1* in spinal cord using qPCR and found that *NPR1* is expressed in similar amounts (Fig. 1F). Together, these results suggest that mouse and human itch neurotransmission likely uses the same signaling molecules.

### A-71915, a mixed NPR1 antagonist/agonist

When the gene for *Nppb* is eliminated in knockout mice or *Npr1*-expressing spinal neurons are ablated, itch responses are attenuated, suggesting that NPR1 signaling is critical for itch responses (*13*). However, it was reported that A-71915, a relatively potent hNPR1 antagonist (*18*), does not block acute itch responses (*22*). An explanation for this may be that A-71915 does not effectively block itch in vivo. As the pharmacodynamic interactions of A-71915 with mNPR1 have not been tested, we developed a method to measure inhibition of mNPR1 by A-71915.

Given that the NPR1 receptor is a ligand-dependent GC (*17*), we reasoned that monitoring agonist-induced changes of intracellular cyclic guanosine monophosphate (cGMP) amounts would be a straightforward way to examine NPR1 inhibition. To measure the production of cGMP by NPR1, we used a circular permutated *Firefly* luciferase molecule that was functionally linked to the cGMP binding domain of human phosphodiesterase 5 [GloSensor technology pGS-40F, (*27*)]. This reporter, together with a luciferase substrate (GloSensor reagent) and a sensitive method for detection of luciferase activity (light emission), permitted us, in real time, to measure cGMP in cells (Fig. 2A). We expressed the cGMP sensor in human embryonic kidney (HEK) 293 cells and examined luciferase activity after stimulation with the nitric oxide donor sodium nitroprusside (SNP), which activates ubiquitously expressed soluble GC (Fig. 2B). As expected, SNP generated a long-lasting increase in luciferase activity. In contrast, stimulation of cGMP reporter cells with hNPPA, hNPPB, and NPPC did not increase cGMP (Fig. 2B), indicating that HEK-293 cells do not express detectable endogenous NP receptors. Next, we transiently expressed *mNpr1* and cGMP sensor in HEK-293 cells and examined receptor activation. As expected, mNPPA, mNPPB, and NPPC dose-dependently increased reporter activity and had stimulation potencies similar to those previously reported (Fig. 2C) (*17*), and as previously reported for hNPR1 (*18*), A-71915 inhibited NP-induced mNPR1 activity (Fig. 2D). In addition, our results showed that A-71915, in the absence of NP, evoked a dose-dependent activation of mNPR1, indicating that, instead of being a neutral antagonist as described for hNPR1 (*18*), A-71915 acted as a partial agonist (Fig. 2E).

### Identification of novel hNPR1 antagonists

Next, we searched for molecules with good antagonistic properties to investigate whether inhibition of NPR1 is a viable approach for alleviating itch. We used a quantitative high-throughput screening (qHTS) method to identify candidate molecules able to inhibit NPR1 from a large chemical library. With a few modifications, we used the same cell-based approach to perform qHTS as we used to determine the properties of A-71915. To increase sensitivity and allow miniaturization to a 1536-well format, we developed a stable cGMP sensor cell line expressing hNRP1, a control cell line with stable expression of cGMP sensor, and a hNPR2 cell line (fig. S1). hNPR1-cGMP reporter cells responded to hNPPA, hNPPB, and NPPC with appropriate potencies (Fig. 3, A and B), whereas cGMP reporter cells lacked responses to hNPPA, hNPPB, and NPPC but were strongly activated by SNP in a dose-dependent fashion (Fig. 3, C and D). To enable assessment of the inhibition of agonist-induced hNPR1 activity and effects of compounds on basal hNPR1 activity, we performed reads before addition and 30 min after application of agonist (Fig. 3E). To improve identification of active compounds and to assist in ranking compounds, we also conducted primary screens at six log concentrations (*28*). Our final hNPR1 sensor assay was highly consistent; screening of the LOPAC1280 (1280 compounds) and BU-CMD (1838 compounds) libraries gave Z′ factor scores of $0.73 \pm 0.07$ and $0.72 \pm 0.2$, respectively. Our assay also had a low hit rate with these small libraries of compounds, and none of the molecules identified as inhibitors from these small libraries passed counterscreens (data file S1).

For the main qHTS, we used an automated robotic system (*29*) and the National Center of Advancing Translational Sciences Genesis library that consists of a chemically and structurally diverse set of small molecules suited for rapid chemical modification (86,437 compounds screened, data file S2). Compounds that inhibited activity (Fig. 3F) were identified using automated software (*28*). The overall hit rate of our screen was 3.9%. These candidate compounds were prioritized based on their potency, efficacy, and structural relationships, and from all positive compounds, 1408 were judged to be strong candidates for further study (see Materials and Methods for details).

Although we identified compounds on the basis of their inhibition, these compounds might be interfering with components of the assay instead of directly inhibiting hNPR1. Therefore, we used overlapping strategies to eliminate false positives and identify bona fide hNPR1 inhibitors. First, we repeated, at eight concentrations, qHTS assays on all selected compounds, confirming all the selected compounds from our primary screen. Second, we subtracted compounds that interfered directly with luciferase or molecules that were cytotoxic (see Materials and Methods) (*30*). Third, to eliminate compounds that directly block the activity of the cGMP sensor or sequester GloSensor reagent, we tested for the inhibition of luciferase activity upon activation of soluble GC in HEK-cGMP sensor cells (using SNP). These counterscreens eliminated most of the initial candidate compounds (data file S3). Only 15 candidates remained after counterscreens were completed (tables S1 and S2). Figure 4 shows three of these candidates that potently inhibit hNPR1 activity. These compounds inhibited hNPR2 and hNPR1 with similar potency (fig. S2). The compounds JS-5, JS-8, and JS-11 show structural similarity, suggesting a possible common mode of action and potentially a shared binding site for this class of antagonists. To examine cross-reactivity of hNPR1 antagonists further, we investigated whether JS-11 could inhibit the cyclase domain of the structurally similar adenylate cyclase (AC) family of enzymes (*31*). Endogenously expressed in HEK-293 cells, ACs were stimulated with forskolin and amounts of cyclic adenosine monophosphate (cAMP) were measured using a cAMP biosensor [GloSensor technology pGS-22F, (*27*)], using a similar approach to the one we used to measure cGMP. Despite using a dose range of JS-11 that completely inhibited NP-induced hNPR1 activity, ACs were not inhibited (fig. S3). In addition, a screen of the SafetyScreen44 panel of off-target G protein–coupled receptors, transmitter transporters, ion channels, nuclear receptors, and enzymes with clinical reference (*32*) only exposed inhibition of CCKAR and HTR2A, two receptors without clearly defined roles in itch sensation (table S3). Therefore, JS-11 is likely a fairly selective antagonist of NPR1.

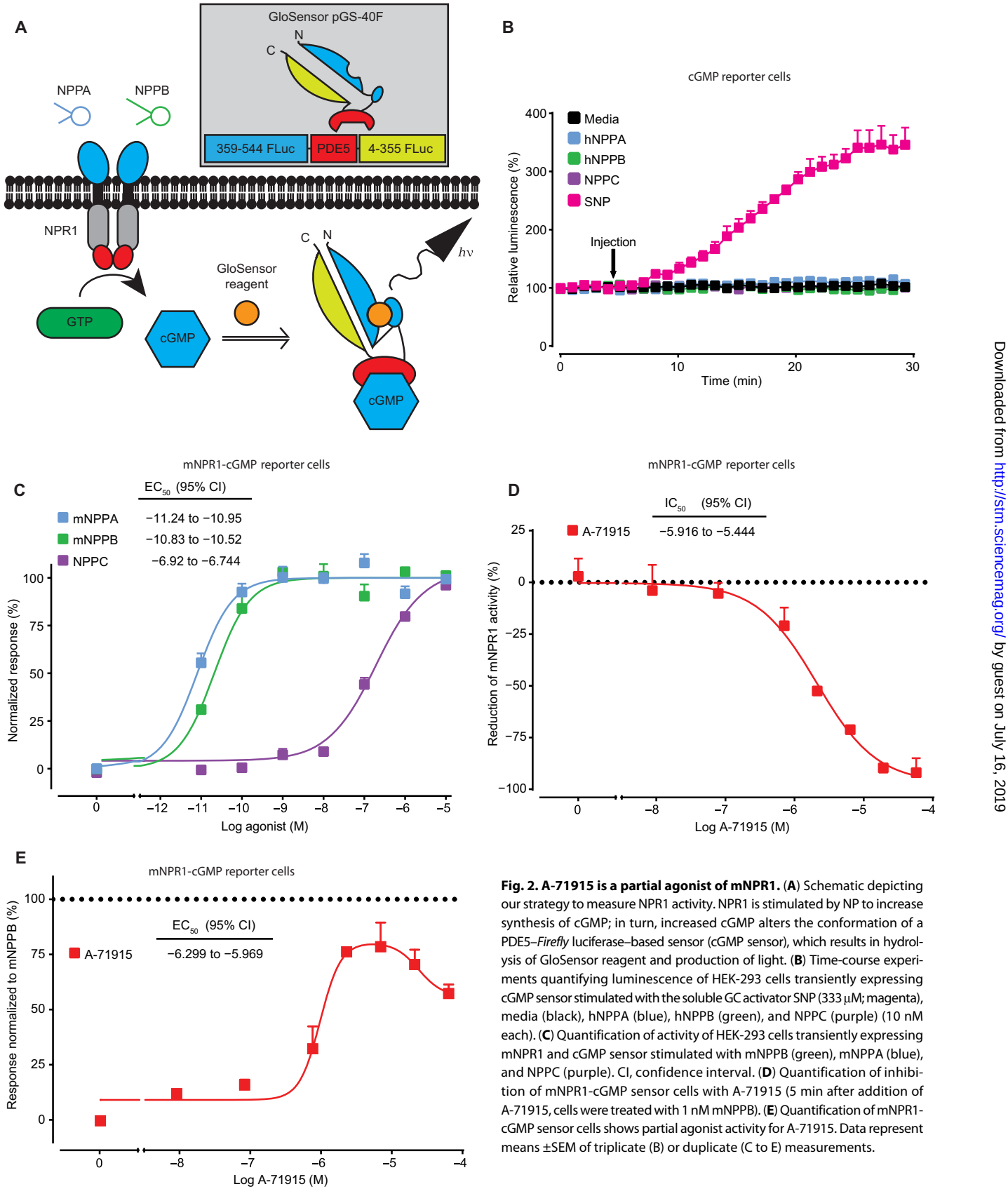


**Fig. 2. A-71915 is a partial agonist of mNPR1.** (**A**) Schematic depicting our strategy to measure NPR1 activity. NPR1 is stimulated by NP to increase synthesis of cGMP; in turn, increased cGMP alters the conformation of a PDE5–*Firefly* luciferase–based sensor (cGMP sensor), which results in hydrolysis of GloSensor reagent and production of light. (**B**) Time-course experiments quantifying luminescence of HEK-293 cells transiently expressing cGMP sensor stimulated with the soluble GC activator SNP (333 μM; magenta), media (black), hNPPA (blue), hNPPB (green), and NPPC (purple) (10 nM each). (**C**) Quantification of activity of HEK-293 cells transiently expressing mNPR1 and cGMP sensor stimulated with mNPPB (green), mNPPA (blue), and NPPC (purple). CI, confidence interval. (**D**) Quantification of inhibition of mNPR1-cGMP sensor cells with A-71915 (5 min after addition of A-71915, cells were treated with 1 nM mNPPB). (**E**) Quantification of mNPR1-cGMP sensor cells shows partial agonist activity for A-71915. Data represent means ±SEM of triplicate (B) or duplicate (C to E) measurements.

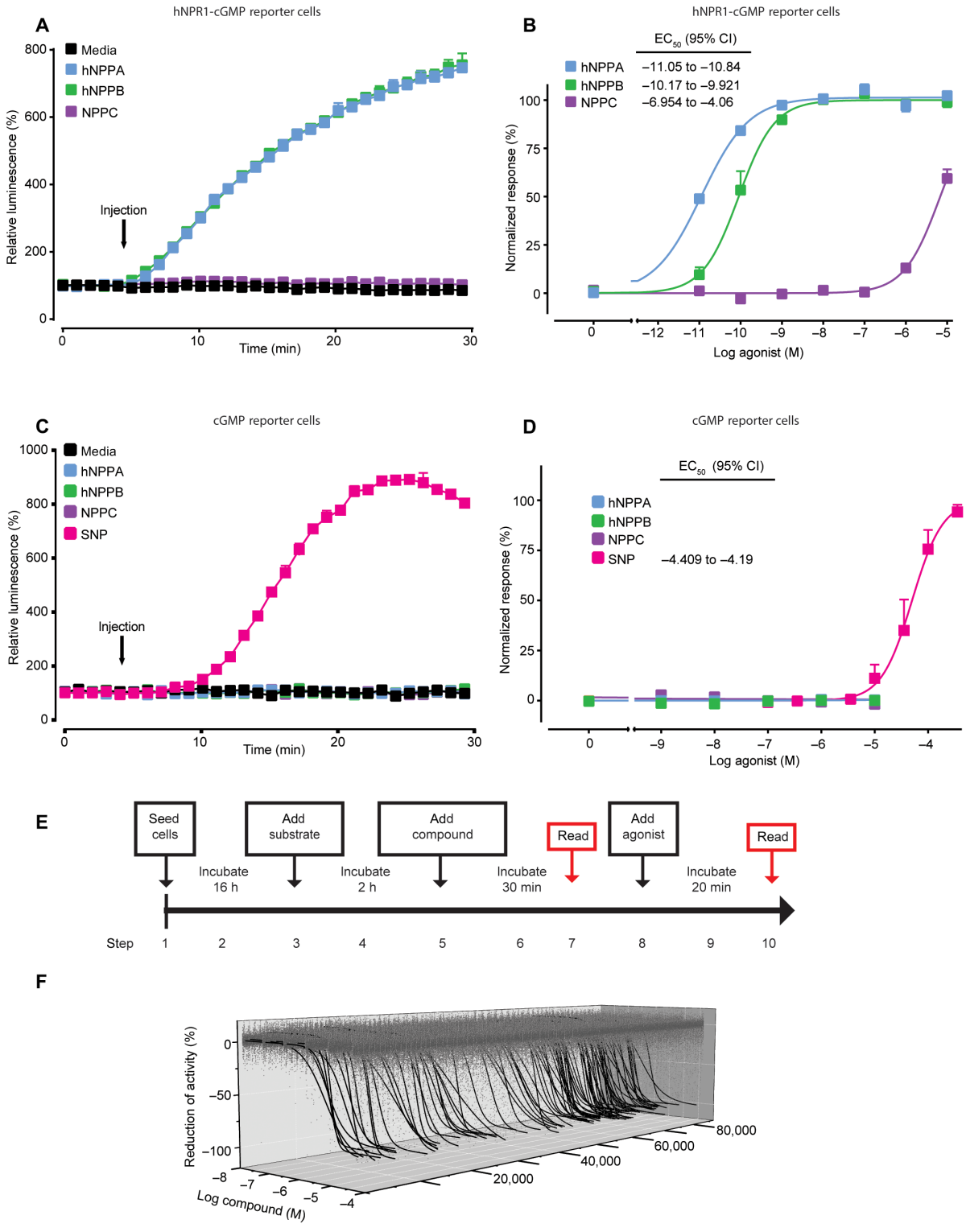


**Fig. 3. Cell-based screen identifies candidate small-molecule inhibitors of hNPR1.** (**A** and **C**) Time-course experiments quantifying luminescence of stable cell lines expressing pGS-40F and hNPR1 (A) and pGS-40F alone (C) stimulated by media (black), hNPPA (blue), hNPPB (green), NPPC (purple) (10 nM each), and SNP (333 μM, magenta). (**B** and **D**) Quantification of activity of HEK-hNPR1-cGMP sensor cells (B) and HEK-cGMP sensor cells (D) with hNPPA (blue), hNPPB (green), NPPC (purple), and SNP (magenta). (**E**) Schematic depicts the time course of our qHTS assay. (**F**) Representative three-axis plot of concentration-response curve profiles for compounds from the Genesis chemical library; 519,417 concentration response values are displayed in gray (1574 outlier values were not plotted). Out of the 3.9% active compounds, 105 compounds with greatest efficacy (maximum antagonism, >90%) are displayed (black traces). Curves were fit using a four-parameter logistic regression. Data represent means ±SEM of duplicate (A to C) or triplicate (D) measurements.

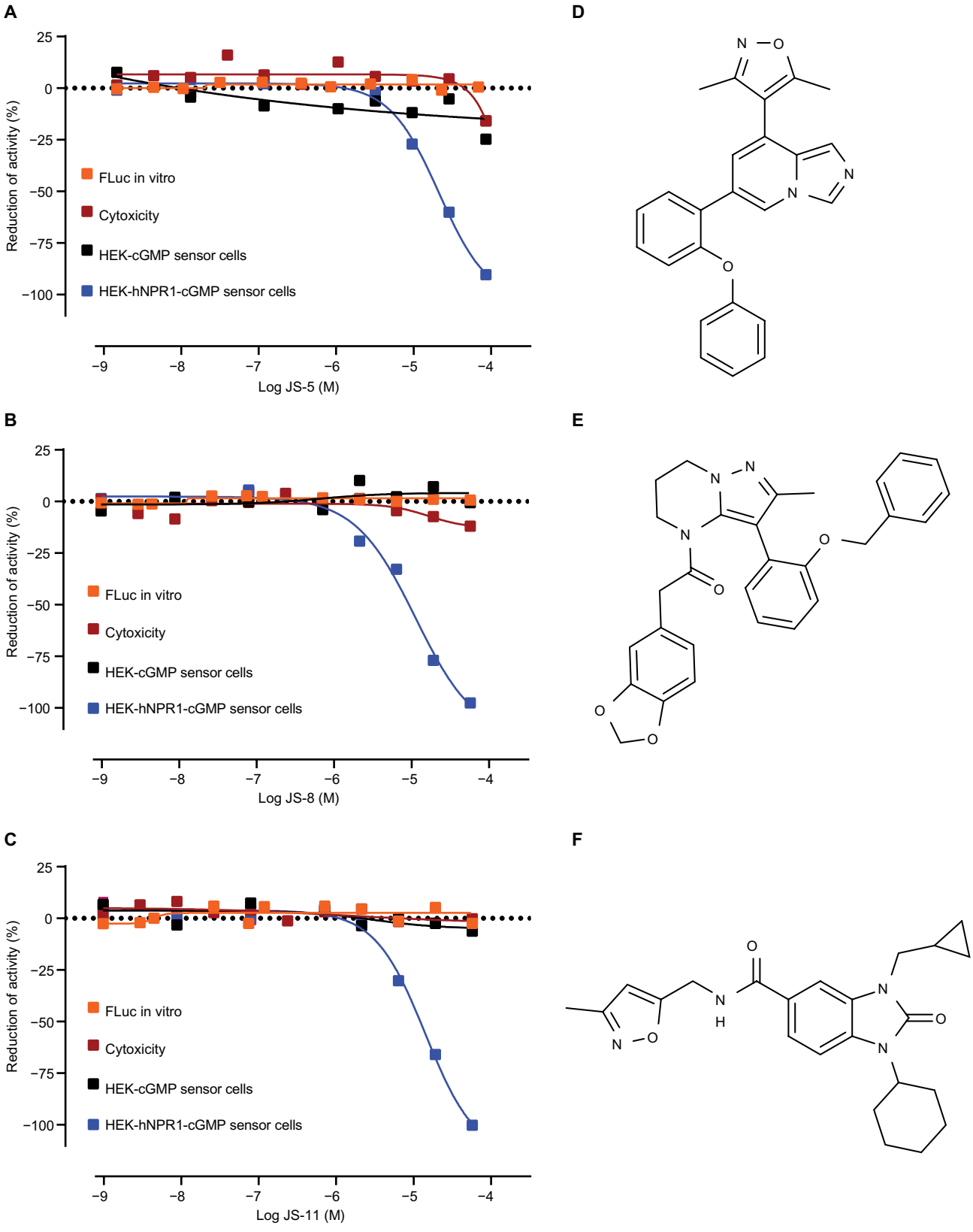


**Fig. 4. Candidate inhibitors attenuate specifically hNPR1 activity.** Quantification of inhibition of hNPR1 activity (blue squares), *Firefly* luciferase activity (orange squares), SNP-induced activity (black squares), and cytotoxicity for HEK-hNPR1-cGMP sensor cells (red squares) by JS-5 (**A**), JS-8 (**B**), and JS-11 (**C**). Data were collected from qHTS assays. (**D** to **F**) Chemical structures of JS-5 (D), JS-8 (E), and JS-11 (F).

### Validation of candidate hNPR1 inhibitors

To study candidate compounds further, we selected 12 molecules from those identified initially that we could obtain in large amounts and at high purity, and we developed an independent strategy to confirm their direct inhibition of hNPR1. The approach we used was to directly determine cGMP production by stimulated hNPR1 in an in vitro assay (Fig. 5A). As expected, we found that the activation of hNPR1 with hNPPA increased cGMP amounts, whereas activation of membranes with SNP did not (Fig. 5B). All tested hNPR1 antagonists blocked cGMP production by hNPR1 (table S4 and Fig. 5C). The recorded potencies of inhibition in the in vitro and cell-based assays, when corrected for differences in assay sensitivity, were very similar (table S5).

We found that both the basal and agonist-induced hNPR1 activities were inhibited by antagonists (Fig. 6A). Because A-71915 does not inhibit basal hNPR1 activity, this suggested to us that the antagonists we identified inhibit hNPR1 activity via a different mechanism. To explore this further, we measured, with fixed concentrations of A-71915, JS-5, JS-8, and JS-11, receptor activity to increasing concentrations of hNPPA. Whereas A-71915 induced a right shift in hNPPA potency without any effect on maximal efficacy, our antagonists reduced maximal responses even at extremely high hNPPA concentrations [$10^5$-fold higher than the half maximal effective concentration ($EC_{50}$)] (Fig. 6B). This apparent lack of effect of increased agonist concentrations could either indicate a noncompetitive inhibition of hNPR1 or be explained by slow dissociation of antagonists from

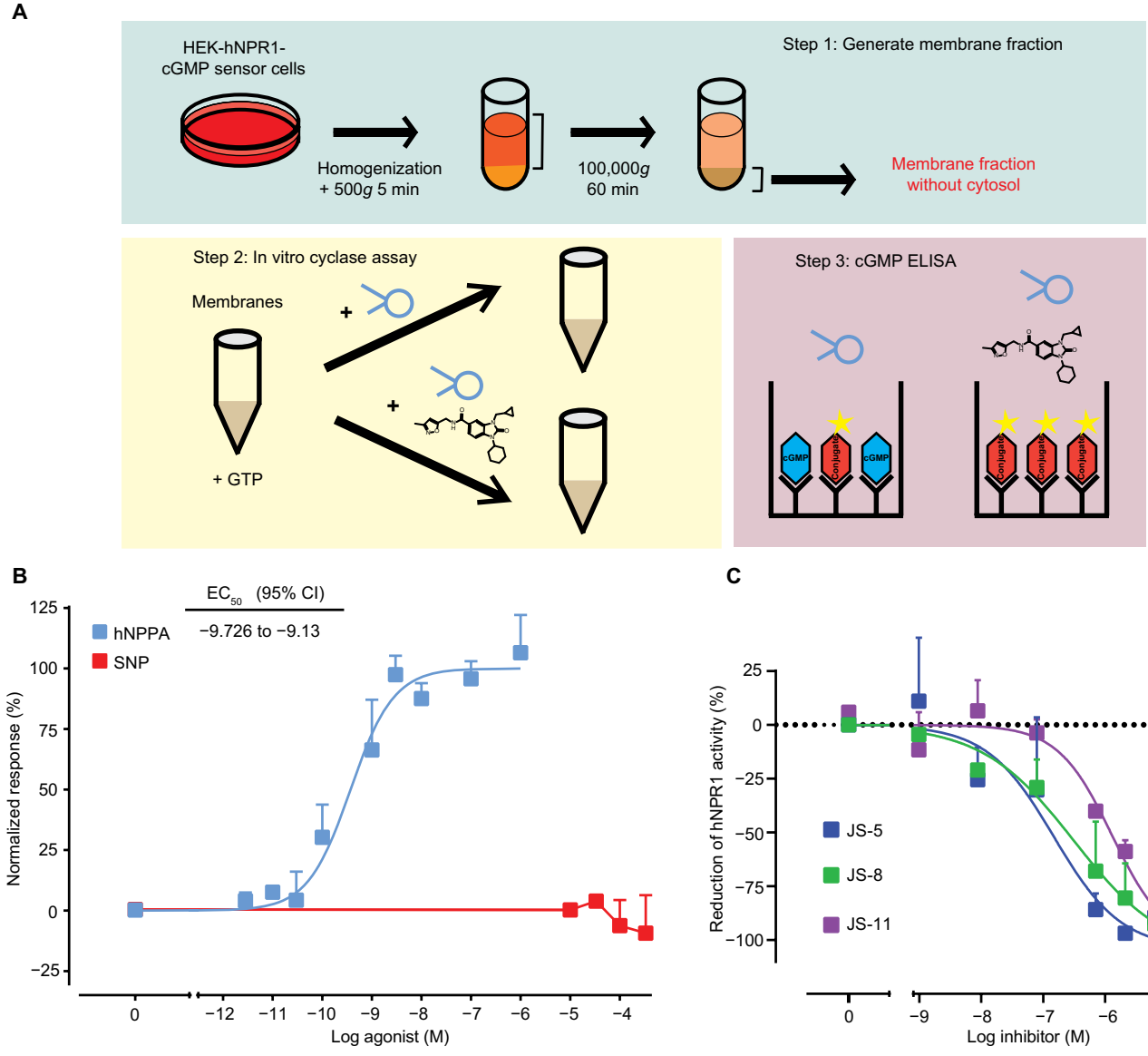


**Fig. 5. Cell-free membrane cyclase assay confirms that candidate compounds are specific antagonists of hNPR1.** (**A**) Schematic depicts our strategy to measure hNPR1 activity with an in vitro assay. A crude membrane fraction was prepared from HEK-hNPR1-cGMP sensor cells. Incubation of hNPR1 membranes with guanosine triphosphate (GTP) and NP results in production of cGMP, and cGMP was measured using an enzyme-linked immunosorbent assay (ELISA) test. (**B**) Quantifications of cGMP production by hNPR1 membranes, stimulated by hNPPA (blue) and SNP (red). (**C**) Quantification of inhibition of hNPPA-stimulated (1 nM) hNPR1 activity by JS-5 (blue), JS-8 (green), or JS-11 (purple). Data represent means ±SEM for triplicate (B, hNPPA), duplicate (B, SNP), and duplicate measurements (C).

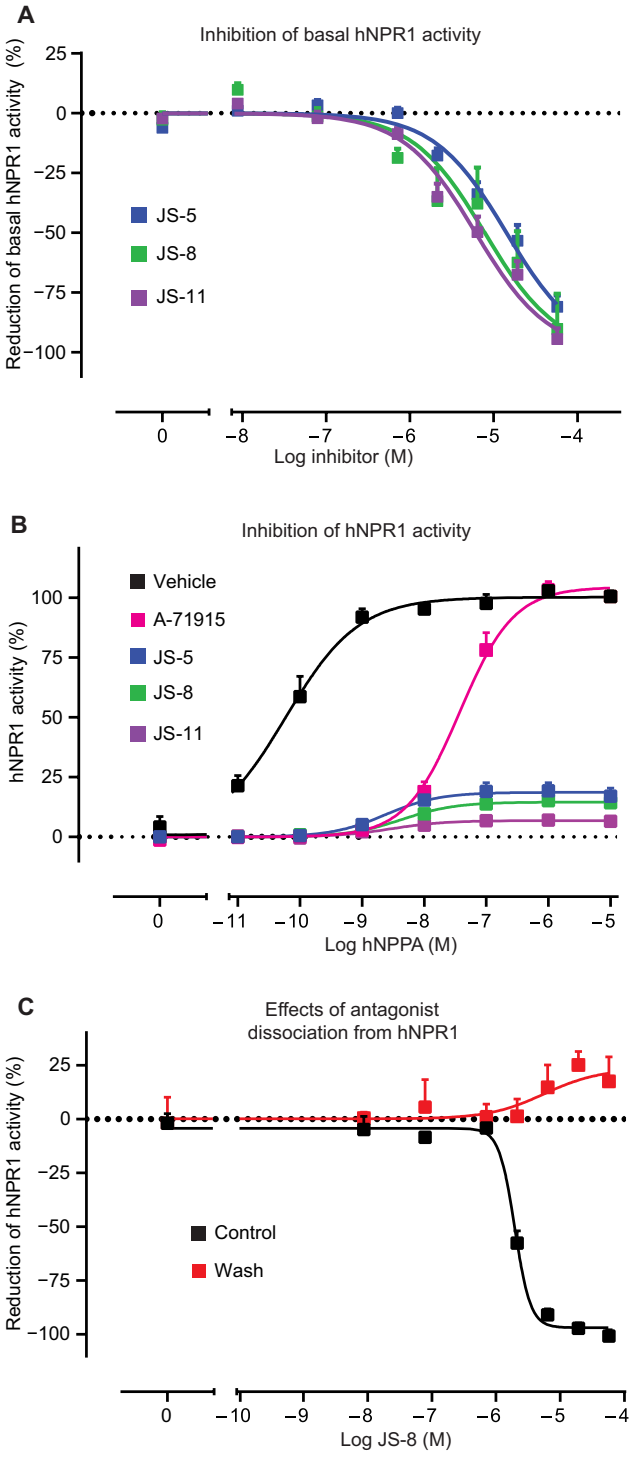


**Fig. 6. hNPR1 antagonists inhibit receptor activity through a noncompetitive mechanism.** (**A**) Quantification of the inhibition of basal hNPR1 activity by antagonists, JS-5 (blue), JS-8 (green), and JS-11 (purple). (**B**) Quantification of hNPR1 activity to increasing concentrations of hNPPA in the presence of a fixed concentration of antagonists (5 μM): JS-5 (blue), JS-8 (green), JS-11 (purple), A-71915 (magenta), and saline (black). (**C**) Quantification of antagonist dissociation from hNPR1. HEK-hNPR1-cGMP sensor cells were treated with JS-8 and either were given a 5-min washing step (red) or were not treated (black). Next, cells were stimulated with hNPPA (60 pM) to test whether JS-8 dissociates rapidly from hNPR1. Data represent means ± SEM of triplicate (A and C) and duplicate (B) measurements.

hNPR1. The latter explanation would mean that washing hNPR1 membranes, after incubation with antagonist, should have little effect on receptor inhibition. To examine this possibility, we added the antagonist JS-8 and measured inhibition of hNPPA-induced hNPR1 activation before and after washing. We found that even a single 5-min washing step was sufficient to completely recover hNPR1 activity (Fig. 6C), suggesting that the antagonists we identified have fast dissociation rates. Therefore, the antagonists we identified probably block hNPR1 via a noncompetitive mechanism.

### Inhibition of itch in vivo by NPR1 antagonists

As we finally wanted to test whether inhibition of NPR1 can alleviate itch in mouse models, we next examined the potencies of inhibition of compounds on mNPR1 (table S6). Comparison of inhibition of hNPR1 and mNPR1 revealed, when corrected for differences in assay sensitivity, that most of the identified compounds had similar inhibitory properties at mouse and human receptors (table S5), suggesting that they might block behavioral responses to itch-inducing agents in vivo in mice.

Because NPR1 signaling has been suggested to be critical for acute itch (*13*), we first sought to investigate the ability of NPR1 antagonists to inhibit acute itch responses. We determined that compound JS-11 might be suited to block itch in vivo because it has a relatively high water solubility and membrane permeability and a reasonable half-life (table S7). Next, we examined the pharmacokinetic properties of JS-11 in vivo. We found that, after intraperitoneal delivery (5 mg/kg), JS-11 concentrations decayed with first-order kinetics in plasma and central nervous system (CNS) tissues with half-life of about 30 min and JS-11 readily crossed the blood-brain barrier (fig. S4) (*33*). Amounts of JS-11 in the CNS reached concentrations that should, based on the calculated $K_i$ (inhibition constant), inhibit mNPR1. JS-11 did not have major untoward effects on mouse behavior when administered intraperitoneally (163 μg, ~7.5 mg/kg), did not alter spontaneous locomotor activity, and did not change rotarod performance (fig. S5, A to C). Next, we tested whether scratching responses induced by intradermal injections of histamine were attenuated by JS-11 (Fig. 7A). Treatment with JS-11 reduced scratching responses to histamine by more than a half (Fig. 7B and fig. S5D). To corroborate this result, we assayed whether JS-11 can inhibit itch responses induced by a second agent that elicits scratching in mice, CYM5442, which activates sphingosine-1-phosphate receptor 1 (*26*). Our results showed that JS-11 attenuates CYM5442-induced scratching (Fig. 7C and fig. S5E).

Previously, we showed that itch can be attenuated by ablation of spinal cord *Npr1* neurons (*13*). To examine whether JS-11 inhibits itch through a spinal cord pathway, we examined pruritogen-activated c-FOS expression in spinal cord neurons (*34*). Corroborating that JS-11 likely inhibits this pathway, JS-11 substantially reduced the number of c-FOS–positive neurons to intradermal histamine challenge (Fig. 7, D to F). In addition, intrathecal delivery of JS-11 (16.3 μg, ~0.75 mg/kg) strongly reduced scratch responses of histamine-challenged mice (Fig. 7G and fig. S5F).

For NPR1 antagonists to have translatable potential, NPPB should also be required for human itch. Although it is not formally possible to directly test this requirement in humans (at this stage), a precondition for NPPB to have a role in human itch neurotransmission would be that it should be expressed in the appropriate sensory neurons. We showed that *NPPB* is expressed in a subset of human *TRPV1* sensory neurons (Fig. 1), but we wondered if it is also coexpressed

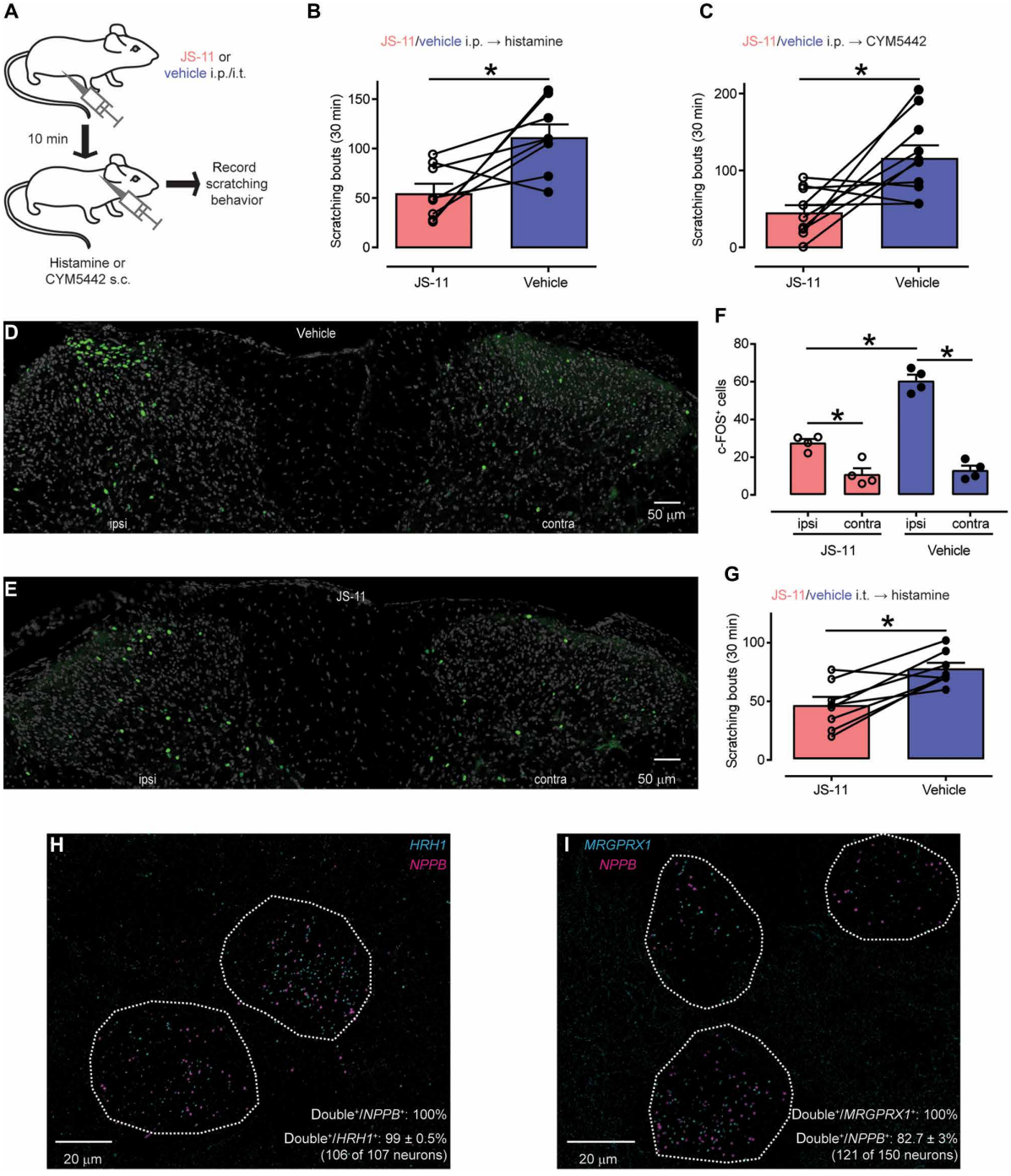


**Fig. 7. NPR1 antagonist inhibits acute itch behavior.** (**A**) Schematic depicting the strategy used to test effects of JS-11 in a mouse model of acute itch. i.p., intraperitoneal; i.t., intrathecal; s.c., subcutaneous. (**B** and **C**) Quantification of scratching responses to histamine (B, $n = 8$) and CYM5442 (C, $n = 10$) (B, $^*P = 0.0221$; C, $^*P = 0.0128$, paired $t$ test). Mice were intraperitoneally injected with 163 μg of JS-11 or vehicle and, 10 min later, injected into the nape of the neck with pruritogens (100 μg of histamine and 8.9 μg of CYM5442). (**D** and **E**) Representative images of c-FOS immunostaining in the spinal cord after intradermal calf injection of histamine (100 μg) and previous administration of JS-11 (163 μg) or vehicle [20% dimethyl sulfoxide (DMSO)]. (**F**) Quantification of the number of c-FOS–positive neurons (average from six sections for each animal; $n = 4$ mice per treatment). Significant differences were assessed using one-way ANOVA and Sidak's multiple comparisons post hoc test. JS-11 reduced the number of spinal c-FOS–positive neurons ipsilateral (ipsi) to the histamine injection ($^*P < 0.0001$) without affecting basal activity on the contralateral (contra) side (ns, $P = 0.9953$). Histamine significantly increased numbers of c-FOS neurons ipsilateral to the injection side in both treatment groups (JS-11, $^*P = 0.0058$; vehicle, $^*P < 0.0001$). (**G**) Quantification of the effect of intrathecal delivery of JS-11 (16.3 μg) and vehicle (20% DMSO) on numbers of scratching bouts to histamine (100 μg into the nape of the neck). Itch responses were significantly reduced by administration of JS-11 ($^*P = 0.0030$, paired $t$ test; $n = 8$). (**H** and **I**) Representative double ISH images of human DRG sections revealed neurons stained for *NPPB* (H and I, magenta), *HRH1* (H, cyan), and *MRGPRX1* (I, cyan). Neurons positive for *NPPB* and itch receptors are highlighted with white dotted profiles.

with known itch receptors. Therefore, we performed double-label ISH on human DRG sections with *NPPB* and the histamine receptor *HRH1* (*35*) and chloroquine receptor *MRGPRX1* (*12*, *36*). We found that *HRH1* is largely coexpressed with *NPPB* [Fig. 7H; 99 ± 0.5% of *HRH1* neurons express *NPPB* (106 of 107 neurons, $n = 4$ donors); all *NPPB* neurons express *HRH1*] and that all *MRGPRX1*-positive cells coexpress *NPPB* (Fig. 7I; 121 *MRGPRX1* neurons express *NPPB*, $n = 4$ donors), although some *NPPB*-expressing cells were *MRGPRX1* negative (17.3 ± 3%; 29 neurons; $n = 4$ DRG donors).

A potential concern with NPR1 antagonists is the known vasodilatory effects of these receptors (*37*), which could potentially produce unwanted cardiovascular effects. To investigate this possible side effect, we examined effects of acute intraperitoneal injection of JS-11 on blood pressure and heart rate. Figure S6 shows that, except for a slight change in the kinetics of a transient (<5 min) drop in blood pressure directly after injection, we could not detect drug-induced changes in either blood pressure or heart rate.

Clinically, most acute itch can be controlled with antihistamines (*1*); however, antihistamines lack effectiveness against persistent forms of itch (*2*, *3*). In different skin disorders associated with persistent itch, including atopic and contact dermatitis, T cell–derived interleukin-31 (IL-31) has been postulated to be a mediator for disease progression and correlated with disease severity in humans (*38*–*41*). Therefore, we examined the expression of *NPPB* with *IL31RA*. Like for *HRH1* and *MRGPRX1* itch receptors, ISH revealed that most of the human *NPPB* neurons coexpress *IL31RA* [Fig. 8A; 90 ± 3% of *IL31RA* neurons express *NPPB* (119 of 126, $n = 4$ donors); all *NPPB* neurons express *IL31RA*]. To further investigate the significance of this coexpression in vivo, we tested the potential for blocking IL-31–mediated itch (*42*) with a NPR1 antagonist in a model of contact hypersensitivity (Fig. 8B). If NPPB is an important mediator of this type of itch, then we anticipated that a NPR1 antagonist would attenuate scratching. In this model, scratching, but not skin inflammation, is dependent on IL-31 (*42*). In line with this notion, as assessed by measuring ear thickness after hapten challenge, acute blockade of NPR1 with JS-11 had no effect on skin inflammation (Fig. 8C). By contrast, JS-11 attenuated hapten-induced scratching responses by about a half (Fig. 8D and fig. S7). This result indicates that ongoing peripheral drive contributes to pruritus in a model of persistent inflammatory dermatitis and suggests that antagonism of NPR1 might be an approach to treat chronic itch.

## DISCUSSION

Chronic itch is a major concern for large numbers of people, particularly because most available treatments are, at best, only partially effective (*3*). Scratching associated with itch is often the principal relief for patients, and this leads long term to severe skin damage. In addition, these skin abrasions are disfiguring and can lead to infections, and this itch scratch cycle seriously reduces quality of life for sufferers. The underlying molecular and cellular mechanisms for itch have started to be understood in mice and other model organisms (*4*, *7*, *43*). In turn, this has led to the possibility of targeting, for the development of new treatments, key signaling molecules. For instance, small-molecule antagonists for gastrin-releasing peptide receptor, a neurotransmitter receptor required for itch (*44*), have been developed (*45*, *46*). Here, in proof-of-principle studies, we examined whether inhibition of the signaling through another crucial neurotransmitter, NPPB, might be a viable method to reduce itch.

The initial rationale for choosing NPPB as a target for the treatment of itch was based on the knowledge of its critical importance for acute itch responses to multiple itch-inducing compounds in mice (*13*). In addition, the expression of *Nppb* in the skin was shown to be markedly increased in models of itch (*16*, *47*, *48*) as well as in patients diagnosed with atopic dermatitis or psoriasis (*16*, *49*), suggestive of involvement of NPPB in persistent itch. Furthermore, in renal failure, a condition known for a high incidence of itch (*50*), blood NPPB concentrations were found to be elevated in human subjects and correlated with itch ratings (*51*). We show that *NPPB* is expressed in a subset of *TRPV1*-expressing human DRG neurons and is coexpressed with the itch receptors *HR1R* and *MRGPRX1* (*36*, *52*). In addition, we find that *IL31RA*, a key player for the development of inflammatory skin diseases associated with chronic itch (*38*–*41*), is coexpressed with *NPPB* in human DRG neurons. For the most part, this expression pattern and other characteristics of human *NPPB* neurons are reminiscent of those in mouse, suggesting that NPPB probably plays a similar function in humans and mice (*13*). Our data also point to an interesting distinction between mice and humans; whereas in mice *Mrgpra3* and *Mrgprc11*, receptors that share some pharmacological similarities with the human MRGPRX1 (*25*), are not coexpressed with *Nppb* (*15*), *MRGPRX1* and *NPPB* are coexpressed in humans.

Given that NPPB is a potential target for development of treatments of itch, we searched for potent NPR1 antagonists. Initially, we tested the previously identified NPR1 inhibitor A-71915 and found that it is a strong partial agonist, not a neutral antagonist, of mNPR1. Because A-71915 is structurally related to NP (*18*), it likely competes with NP for the same binding site. This domain is the least conserved region of murine and hNPR1, potentially explaining this species-specific difference in pharmacodynamics. The fact that A-71915 is not a neutral antagonist, but is instead a strong partial agonist, suggests a potential explanation for the lack of efficacy of A-71915 on itch behavior in vivo (*22*). Also, A-71915 may have a very short half-life in humans (*53*–*56*). For these reasons, we embarked on HTS to identify novel NPR1 antagonists that can better inhibit NPR1 activity. Our HTS identified 15 new hNPR1 antagonists. Although these molecules efficiently inhibited both human and mNPR1, they also inhibited hNPR2 and, at least for JS-11, inhibited CCKAR and HTR2A. In future studies, this information may be helpful in identifying more specific NPR1 antagonists. Pharmacological analysis of antagonists revealed that they likely act as noncompetitive inhibitors of NPR1. Similar but oppositional allosteric effects on NPR1 activity have been described before (*57*, *58*). In particular, binding of a chloride ion to a region of the extracellular domain that is not directly involved in ligand binding favored NPPA binding to NPR1 (*58*), and binding of adenosine triphosphate to the intracellular kinase homology domain increased NPPA-induced NPR1 activation (*57*). Although the exact molecular mechanism of NPR1 inhibition by our antagonists is unknown, it might involve interference with one or more steps of the sequential ligand-induced NPR1 activation cascade. Upon binding of NP to the orthosteric binding site, which is built asymmetrically by two NPR1 molecules, a twisting motion is thought to be induced (*59*). This, in turn, leads to activation of the intracellular GC domain (*59*). However, because structural data are lacking for the intracellular domains of NPR1 (*60*, *61*), it is unclear which exact structural reconfigurations of the NPR1 intracellular domains are involved. We note that there are some common structural elements to the inhibitors we identified. For example, the

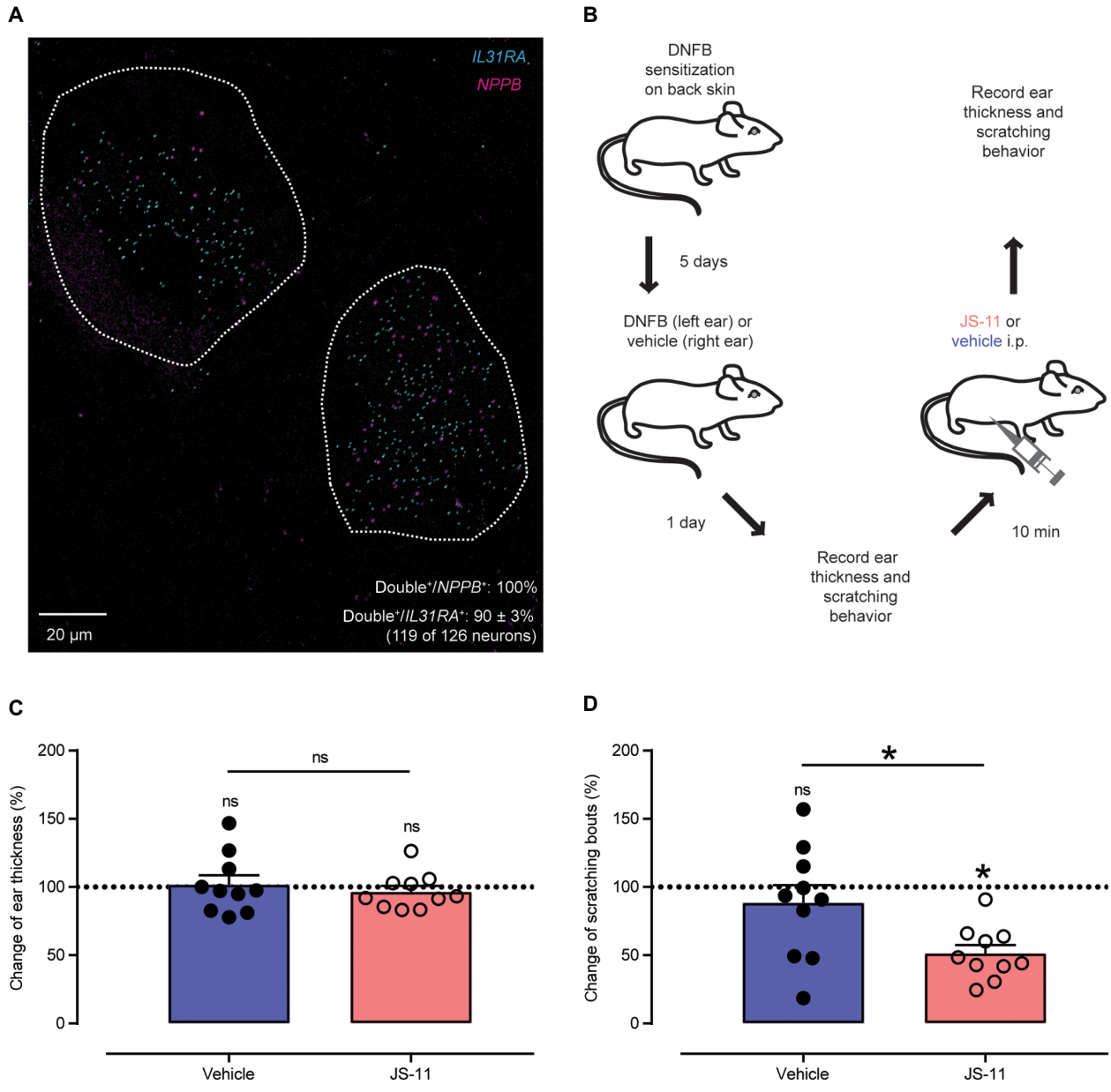


**Fig. 8. NPR1 antagonism inhibits itching in a mouse model of contact dermatitis.** (**A**) Representative double ISH image of a human DRG section reveals that *NPPB* (magenta) and *IL31RA* (cyan) are coexpressed. Neurons coexpressing *NPPB* and *IL31RA* are highlighted with white dotted profiles. (**B**) Schematic depicts the experimental strategy to examine the effects of JS-11 on a mouse model of contact hypersensitivity-induced itch. (**C**) Quantification of the effects of JS-11 treatment on contact dermatitis–induced changes in ear thickness. There were no significant differences between JS-11 (pink, 163 μg) and vehicle (blue, 20% DMSO) groups ($n = 10$). Ear thickness was analyzed using one-sample *t* test against a theoretical mean of 100% (vehicle: ns, $P = 0.8020$ and JS-11: ns, $P = 0.4384$), and differences between treatment groups were assessed using unpaired *t* test (ns, $P = 0.5283$). (**D**) Quantification of the effects of JS-11 treatment on contact dermatitis–induced changes in scratching responses. Itch behavior was significantly reduced by administration of JS-11 (pink, 163 μg) compared to vehicle (blue, 20% DMSO) ($n = 10$). Scratching responses were analyzed using one-sample *t* test against a theoretical mean of 100% (vehicle: ns, $P = 0.3951$ and JS-11: $^*P < 0.0001$), and differences between treatment groups were assessed using unpaired *t* test ($^*P = 0.0193$).

nitrogen-containing indene cores in JS-5, JS-8, and JS-11 may embody structural features of adenosine or guanosine triphosphate sufficient for occupancy of the nucleotide-binding site(s) conserved in NPR1 and NPR2, thus explaining the noncompetitive nature of NP antagonism and equivalent NPR subtype selectivity observed. However, our findings that ACs are not inhibited by JS-11 suggest that these antagonists are not broad cyclase inhibitors (*31*).

In the present study, we found that blocking NPR1 not only is effective in attenuating acute itch but also reduced scratching in a model for persistent inflammatory dermatitis that is associated with chronic itch. At this point, we cannot exclude the possibility that the itch-reducing effects of JS-11 may, at least in part, be caused by inhibition of off-targets. However, this is very unlikely, as NPR2, CCKAR, and HTR2A have not been associated with histamine- or

CYM5442-induced itch or with spontaneous itch in persistent inflammatory dermatitis. Based on previous reports of the mechanism by which NPPB acts (13), we propose that the site of action of JS-11 is the *Npr1*-expressing interneurons in the spinal cord. Consistent with this, JS-11 readily crosses the blood-brain barrier and reaches concentrations that, based on our in vitro characterization, predict mNPR1 inhibition. Also, we found that intrathecal delivery of JS-11 phenocopied the same itch-attenuating effects of systemic administration, and pruritogen-induced activation of spinal dorsal horn neurons was likewise reduced by JS-11.

As well as being expressed in spinal interneurons, NPR1 is expressed in other tissues, including the kidney and vasculature (*37*), raising concerns about potential unwanted side effects of NPR1 inhibition. We measured cardiovascular effects of JS-11 after acute delivery as a test of preclinical safety. In this acute setting, we did not find major effects on blood pressure or heart rate. This lack of effect may be because the JS-11 dose we used did not suppress cardiovascular effects of NPPA, the most potent agonist of NPR1, as efficiently as the pruritic effects of NPPB. Future studies are needed to systematically examine all possible potential side effects of NPR1 antagonists, especially under chronic NPR1 inhibition. However, NPR1 inhibition may still be practical in renal failure patients because one of the major sites of action of NP is the kidney. Because uremic itch affects a large percentage of kidney failure patients and there are few effective treatments, an anti-itch drug would considerably improve the quality of life for this growing patient population (*50*).

There are limitations of translatability to the clinic of NPR1 antagonism and using JS-11 to alleviate itch. The investigational inhibitor JS-11 is not suitable for use in the clinic because of its relatively low affinity, issues of cross-reactivity, and insufficient physicochemical properties. Furthermore, NPR1 inhibition may remain problematic because of unwanted on-site effects. In addition, preclinical tests in large animals that include a thorough mechanistic investigation of JS-11 effects need to be conducted. However, although there are additional steps and hurdles before NPR1 antagonists might be used for the treatment of itch, our data suggest that NPR1 might be a potential target for treating acute and chronic itch.

## MATERIALS AND METHODS

### Study design

The primary research objective was to determine if itch could be reduced by antagonism of the NPPB receptor NPR1. All other hypotheses were related to this objective. The research subjects and units of investigation were cell culture cells, DRG and spinal cord tissue from human donors, and mice in controlled laboratory experiments. Animals were randomly assigned to two groups, and the experimenter was not blinded. Sample sizes for in vitro and cell-based assays were those used by other laboratories in the field. For animal experiments, sample sizes were based on experience and were of a size generally used in the itch field. Data from two mice (Fig. 7B) were excluded, as these mice did not complete testing because they were euthanized for reasons unconnected with the experiment.

### Statistical analysis

All data are shown as the mean ± SEM, and statistical analyses were performed with Prism 7.0. To determine whether samples were normally distributed, D'Agostino & Pearson ($n > 7$) or Shapiro-Wilk ($n < 7$) tests were performed. Differences between mean values of two groups were analyzed using unpaired or paired two-tailed *t* test or two-tailed Mann-Whitney or Wilcoxon test. Mean differences of more than two groups were analyzed using one-way analysis of variance (ANOVA) with Sidak's multiple comparisons post hoc test or Friedman's test with Dunn's multiple comparisons post hoc test. Differences in scratching time-course experiments were analyzed with two-way ANOVA and Sidak's multiple comparisons post hoc test. Differences were considered significant for $^*P < 0.05$. Exact *P* values and definition and number of replicates are given in the respective figure legend.

## SUPPLEMENTARY MATERIALS

stm.sciencemag.org/cgi/content/full/11/500/eaav5464/DC1
Materials and Methods
Fig. S1. Generation of HEK-hNPR2-cGMP sensor cells.
Fig. S2. hNPR1 inhibitors also block hNPR2.
Fig. S3. JS-11 does not inhibit ACs.
Fig. S4. In vivo pharmacokinetics of JS-11.
Fig. S5. Effects of NPR1 antagonist on general motor behavior and itch responses.
Fig. S6. JS-11 does not cause extensive cardiovascular side effects.
Fig. S7. JS-11 inhibits itching in a mouse model of contact dermatitis.
Fig. S8. General plate map layout for qHTS.
Fig. S9. qHTS concentration response curves for JS-1 through JS-15.
Table S1. Summary of qHTS and counterscreens.
Table S2. Corroboration of hNPR1 inhibition in screening assay.
Table S3. SafetyScreen44-dependent test for off-targets of JS-11.
Table S4. Inhibition of hNPR1 in membrane cyclase assay.
Table S5. $K_i$ values for hNPR1 and mNPR1.
Table S6. hNPR1 antagonists also inhibit mNPR1.
Table S7. In vitro pharmacokinetics of JS-11 and JS-8.
Table S8. PubChem AIDs deposited and used for this study.
Table S9. Clinical information of human DRG donors.
Data file S1. LOPAC pilot screening data.
Data file S2. Genesis primary qHTS screening data.
Data file S3. qHTS follow-up screening data.
Data file S4. Raw data.
References (*62*–*72*)

## REFERENCES AND NOTES


1. F. Dalgard, Å. Svensson, J. Ø. Holm, J. Sundby, Self-reported skin morbidity in Oslo. Associations with sociodemographic factors among adults in a cross-sectional study. *Br. J. Dermatol.* **151**, 452–457 (2004).
2. S. P. Kini, L. K. DeLong, E. Veledar, A. M. McKenzie-Brown, M. Schaufele, S. C. Chen, The impact of pruritus on quality of life: The skin equivalent of pain. *Arch. Dermatol.* **147**, 1153–1156 (2011).
3. G. Yosipovitch, M. W. Greaves, M. Schmelz, Itch. *Lancet* **361**, 690–694 (2003).
4. D. M. Bautista, S. R. Wilson, M. A. Hoon, Why we scratch an itch: The molecules, cells and circuits of itch. *Nat. Neurosci.* **17**, 175–182 (2014).
5. A. Ikoma, M. Steinhoff, S. Ständer, G. Yosipovitch, M. Schmelz, The neurobiology of itch. *Nat. Rev. Neurosci.* **7**, 535–547 (2006).
6. S. Ständer, E. Weisshaar, T. Mettang, J. C. Szepietowski, E. Carstens, A. Ikoma, N. V. Bergasa, U. Gieler, L. Misery, J. Wallengren, U. Darsow, M. Streit, D. Metze, T. A. Luger, M. W. Greaves, M. Schmelz, G. Yosipovitch, J. D. Bernhard, Clinical classification of itch: A position paper of the International Forum for the Study of Itch. *Acta Derm. Venereol.* **87**, 291–294 (2007).
7. L. Han, X. Dong, Itch mechanisms and circuits. *Annu. Rev. Biophys.* **43**, 331–355 (2014).
8. E. Azimi, J. Xia, E. A. Lerner, Peripheral mechanisms of itch. *Curr. Probl. Dermatol.* **50**, 18–23 (2016).
9. E. Azimi, V. B. Reddy, P. J. S. Pereira, S. Talbot, C. J. Woolf, E. A. Lerner, Substance P activates Mas-related G protein-coupled receptors to induce itch. *J. Allergy Clin. Immunol.* **140**, **e443**, 447–453 (2017).
10. S. R. Wilson, L. The, L. M. Batia, K. Beattie, G. E. Katibah, S. P. McClain, M. Pellegrino, D. M. Estandian, D. M. Bautista, The epithelial cell-derived atopic dermatitis cytokine TSLP activates neurons to induce itch. *Cell* **155**, 285–295 (2013).
11. B. McNeil, X. Dong, Peripheral mechanisms of itch. *Neurosci. Bull.* **28**, 100–110 (2012).
12. Q. Liu, Z. Tang, L. Surdenikova, S. Kim, K. N. Patel, A. Kim, F. Ru, Y. Guan, H. J. Weng, Y. Geng, B. J. Undem, M. Kollarik, Z. F. Chen, D. J. Anderson, X. Dong, Sensory neuron-specific GPCR Mrgprs are itch receptors mediating chloroquine-induced pruritus. *Cell* **139**, 1353–1365 (2009).

13. S. K. Mishra, M. A. Hoon, The cells and circuitry for itch responses in mice. *Science* **340**, 968–971 (2013).
14. L. Han, C. Ma, Q. Liu, H.-J. Weng, Y. Cui, Z. Tang, Y. Kim, H. Nie, L. Qu, K. N. Patel, Z. Li, B. McNeil, S. He, Y. Guan, B. Xiao, R. H. Lamotte, X. Dong, A subpopulation of nociceptors specifically linked to itch. *Nat. Neurosci.* **16**, 174–182 (2013).
15. J. Huang, E. Polgár, H. J. Solinski, S. K. Mishra, P.-Y. Tseng, N. Iwagaki, K. A. Boyle, A. C. Dickie, M. C. Kriegbaum, H. Wildner, H. U. Zeilhofer, M. Watanabe, J. S. Riddell, A. J. Todd, M. A. Hoon, Circuit dissection of the role of somatostatin in itch and pain. *Nat. Neurosci.* **21**, 707–716 (2018).
16. J. Meng, M. Moriyama, M. Feld, J. Buddenkotte, T. Buhl, A. Szollosi, J. Zhang, P. Miller, A. Ghetti, M. Fischer, P. W. Reeh, C. Shan, J. Wang, M. Steinhoff, New mechanism underlying IL-31-induced atopic dermatitis. *J. Allergy Clin. Immunol.* **141**, 1677–1689.e8 (2018).
17. S. P. Alexander, H. E. Benson, E. Faccenda, A. J. Pawson, J. L. Sharman, M. Spedding, J. A. Peters, A. J. Harmar, CGTP Collaborators, The Concise Guide to PHARMACOLOGY 2013/14: Catalytic receptors. *Br. J. Pharmacol.* **170**, 1676–1705 (2013).
18. C. Delporte, J. Winand, P. Poloczek, T. Von Geldern, J. Christophe, Discovery of a potent atrial natriuretic peptide antagonist for ANPA receptors in the human neuroblastoma NB-OK-1 cell line. *Eur. J. Pharmacol.* **224**, 183–188 (1992).
19. Y. Kambayashi, S. Nakajima, M. Ueda, K. Inouye, A dicarba analog of beta-atrial natriuretic peptide (beta-ANP) inhibits guanosine 3′,5′-cyclic monophosphate production induced by alpha-ANP in cultured rat vascular smooth muscle cells. *FEBS Lett.* **248**, 28–34 (1989).
20. W. Weber, W. Fischli, E. Hochuli, E. Kupfer, E. K. Weibel, Anantin—A peptide antagonist of the atrial natriuretic factor (ANF). I. Producing organism, fermentation, isolation and biological activity. *J. Antibiot.* **44**, 164–171 (1991).
21. D. F. Wyss, H. W. Lahm, M. Manneberg, A. M. Labhardt, Anantin—A peptide antagonist of the atrial natriuretic factor (ANF). II. Determination of the primary sequence by NMR on the basis of proton assignments. *J. Antibiot.* **44**, 172–180 (1991).
22. N. Kiguchi, D. D. Sukhtankar, H. Ding, K. Tanaka, S. Kishioka, C. M. Peters, M. C. Ko, Spinal functions of B-type natriuretic peptide, gastrin-releasing peptide, and their cognate receptors for regulating itch in mice. *J. Pharmacol. Exp. Ther.* **356**, 596–603 (2016).
23. X. Dong, S. Han, M. J. Zylka, M. I. Simon, D. J. Anderson, A diverse family of GPCRs expressed in specific subsets of nociceptive sensory neurons. *Cell* **106**, 619–632 (2001).
24. P. M. Lembo, E. Grazzini, T. Groblewski, D. O'Donnell, M.-O. Roy, J. Zhang, C. Hoffert, J. Cao, R. Schmidt, M. Pelletier, M. Labarre, M. Gosselin, Y. Fortin, D. Banville, S. H. Shen, P. Ström, K. Payza, A. Dray, P. Walker, S. Ahmad, Proenkephalin A gene products activate a new family of sensory neuron–specific GPCRs. *Nat. Neurosci.* **5**, 201–209 (2002).
25. H. J. Solinski, T. Gudermann, A. Breit, Pharmacology and signaling of MAS-related G protein–coupled receptors. *Pharmacol. Rev.* **66**, 570–597 (2014).
26. H. J. Solinski, M. C. Kriegbaum, P. Y. Tseng, T. W. Earnest, X. Gu, A. Barik, A. T. Chesler, M. A. Hoon, Nppb neurons are sensors of mast cell-induced itch. *Cell Rep.* **26**, 3561–3573. e4 (2019).
27. F. Fan, B. F. Binkowski, B. L. Butler, P. F. Stecha, M. K. Lewis, K. V. Wood, Novel genetically encoded biosensors using firefly luciferase. *ACS Chem. Biol.* **3**, 346–351 (2008).
28. J. Inglese, D. S. Auld, A. Jadhav, R. L. Johnson, A. Simeonov, A. Yasgar, W. Zheng, C. P. Austin, Quantitative high-throughput screening: A titration-based approach that efficiently identifies biological activities in large chemical libraries. *Proc. Natl. Acad. Sci. U.S.A.* **103**, 11473–11478 (2006).
29. S. Michael, D. Auld, C. Klumpp, A. Jadhav, W. Zheng, N. Thorne, C. P. Austin, J. Inglese, A. Simeonov, A robotic platform for quantitative high-throughput screening. *Assay Drug Dev. Technol.* **6**, 637–657 (2008).
30. S.-W. Jang, C. Lopez-Anido, R. MacArthur, J. Svaren, J. Inglese, Identification of drug modulators targeting gene-dosage disease CMT1A. *ACS Chem. Biol.* **7**, 1205–1213 (2012).
31. R. K. Sunahara, A. Beuve, J. J. Tesmer, S. R. Sprang, D. L. Garbers, A. G. Gilman, Exchange of substrate and inhibitor specificities between adenylyl and guanylyl cyclases. *J. Biol. Chem.* **273**, 16332–16338 (1998).
32. J. Bowes, A. J. Brown, J. Hamon, W. Jarolimek, A. Sridhar, G. Waldron, S. Whitebread, Reducing safety-related drug attrition: The use of in vitro pharmacological profiling. *Nat. Rev. Drug Discov.* **11**, 909–922 (2012).
33. S. A. Hitchcock, L. D. Pennington, Structure-brain exposure relationships. *J. Med. Chem.* **49**, 7559–7583 (2006).
34. A. M. Bell, M. Gutierrez-Mecinas, E. Polgár, A. J. Todd, Spinal neurons that contain gastrin-releasing peptide seldom express Fos or phosphorylate extracellular signal-regulated kinases in response to intradermal chloroquine. *Mol. Pain* **12**, 174480691664960 (2016).
35. W.-S. Shim, U. Oh, Histamine-induced itch and its relationship with pain. *Mol. Pain* **4**, 29 (2008).
36. P. Sikand, X. Dong, R. H. Lamotte, BAM8–22 peptide produces itch and nociceptive sensations in humans independent of histamine release. *J. Neurosci.* **31**, 7563–7567 (2011).
37. L. R. Potter, S. Abbey-Hosch, D. M. Dickey, Natriuretic peptides, their receptors, and cyclic guanosine monophosphate-dependent signaling functions. *Endocr. Rev.* **27**, 47–72 (2006).
38. F. Cevikbas, X. Wang, T. Akiyama, C. Kempkes, T. Savinko, A. Antal, G. Kukova, T. Buhl, A. Ikoma, J. Buddenkotte, V. Soumelis, M. Feld, H. Alenius, S. R. Dillon, E. Carstens, B. Homey, A. Basbaum, M. Steinhoff, A sensory neuron-expressed IL-31 receptor mediates T helper cell-dependent itch: Involvement of TRPV1 and TRPA1. *J. Allergy Clin. Immunol.* **133**, 448–460 (2014).
39. S. Weidinger, N. Novak, Atopic dermatitis. *Lancet* **387**, 1109–1122 (2016).
40. M. M. Neis, B. Peters, A. Dreuw, J. Wenzel, T. Bieber, C. Mauch, T. Krieg, S. Stanzel, P. C. Heinrich, H. F. Merk, A. Bosio, J. M. Baron, H. M. Hermanns, Enhanced expression levels of IL-31 correlate with IL-4 and IL-13 in atopic and allergic contact dermatitis. *J. Allergy Clin. Immunol.* **118**, 930–937 (2006).
41. A. Rabenhorst, K. Hartmann, Interleukin-31: A novel diagnostic marker of allergic diseases. *Curr. Allergy Asthma Rep.* **14**, 423 (2014).
42. A. Takamori, A. Nambu, K. Sato, S. Yamaguchi, K. Matsuda, T. Numata, T. Sugawara, T. Yoshizaki, K. Arae, H. Morita, K. Matsumoto, K. Sudo, K. Okumura, J. Kitaura, H. Matsuda, S. Nakae, IL-31 is crucial for induction of pruritus, but not inflammation, in contact hypersensitivity. *Sci. Rep.* **8**, 6639 (2018).
43. M. A. Hoon, Molecular dissection of itch. *Curr. Opin. Neurobiol.* **34**, 61–66 (2015).
44. Y.-G. Sun, Z.-F. Chen, A gastrin-releasing peptide receptor mediates the itch sensation in the spinal cord. *Nature* **448**, 700–703 (2007).
45. X. Y. Liu, Z. C. Liu, Y. G. Sun, M. Ross, S. Kim, F. F. Tsai, Q. F. Li, J. Jeffry, J. Y. Kim, H. H. Loh, Z. F. Chen, Unidirectional cross-activation of GRPR by MOR1D uncouples itch and analgesia induced by opioids. *Cell* **147**, 447–458 (2011).
46. Y.-G. Sun, Z.-Q. Zhao, X.-L. Meng, J. Yin, X.-Y. Liu, Z.-F. Chen, Cellular basis of itch sensation. *Science* **325**, 1531–1534 (2009).
47. D. A. Ewald, S. Noda, M. Oliva, T. Litman, S. Nakajima, X. Li, H. Xu, C. T. Workman, P. Scheipers, N. Svitacheva, T. Labuda, J. G. Krueger, M. Suarez-Farinas, K. Kabashima, E. Guttman-Yassky, Major differences between human atopic dermatitis and murine models, as determined by using global transcriptomic profiling. *J. Allergy Clin. Immunol.* **139**, 562–571 (2017).
48. B. Liu, Y. Tai, S. Achanta, M. M. Kaelberer, A. I. Caceres, X. Shao, J. Fang, S.-E. Jordt, IL-33/ST2 signaling excites sensory neurons and mediates itch response in a mouse model of poison ivy contact allergy. *Proc. Natl. Acad. Sci. U.S.A.* **113**, E7572–E7579 (2016).
49. L. A. Nattkemper, H. L. Tey, R. Valdes-Rodriguez, H. Lee, N. K. Mollanazar, C. Albornoz, K. M. Sanders, G. Yosipovitch, The genetics of chronic itch: Gene expression in the skin of patients with atopic dermatitis and psoriasis with severe itch. *J. Invest. Dermatol.* **138**, 1311–1317 (2018).
50. S. A. Combs, J. P. Teixeira, M. J. Germain, Pruritus in kidney disease. *Semin. Nephrol.* **35**, 383–391 (2015).
51. Y. Shimizu, A. Sonoda, C. Nogi, Y. Ogushi, R. Kanda, S. Yamaguchi, N. Nohara, T. Aoki, K. Yamada, J. Nakata, H. Io, A. Kurusu, C. Hamada, S. Horikoshi, Y. Tomino, B-type (brain) natriuretic peptide and pruritus in hemodialysis patients. *Int. J. Nephrol. Renovasc. Dis.* **7**, 329–335 (2014).
52. M. G. Davies, M. W. Greaves, Sensory responses of human skin to synthetic histamine analogues and histamine. *Br. J. Clin. Pharmacol.* **9**, 461–465 (1980).
53. P. J. Hunt, A. M. Richards, E. A. Espiner, M. G. Nicholls, T. G. Yandle, Bioactivity and metabolism of C-type natriuretic peptide in normal man. *J. Clin. Endocrinol. Metab.* **78**, 1428–1435 (1994).
54. M. Mukoyama, K. Nakao, K. Hosoda, S. Suga, Y. Saito, Y. Ogawa, G. Shirakami, M. Jougasaki, K. Obata, H. Yasue, Brain natriuretic peptide as a novel cardiac hormone in humans. Evidence for an exquisite dual natriuretic peptide system, atrial natriuretic peptide and brain natriuretic peptide. *J. Clin. Invest.* **87**, 1402–1412 (1991).
55. K. Nakao, A. Sugawara, N. Morii, M. Sakamoto, T. Yamada, H. Itoh, S. Shiono, Y. Saito, K. Nishimura, T. Ban, K. Kangawa, H. Matsuo, H. Imura, The pharmacokinetics of alpha-human atrial natriuretic polypeptide in healthy subjects. *Eur. J. Clin. Pharmacol.* **31**, 101–103 (1986).
56. T. G. Yandle, A. M. Richards, M. G. Nicholls, R. Cuneo, E. A. Espiner, J. H. Livesey, Metabolic clearance rate and plasma half life of alpha-human atrial natriuretic peptide in man. *Life Sci.* **38**, 1827–1833 (1986).
57. L. K. Antos, S. E. Abbey-Hosch, D. R. Flora, L. R. Potter, ATP-independent activation of natriuretic peptide receptors. *J. Biol. Chem.* **280**, 26928–26932 (2005).
58. K. S. Misono, Atrial natriuretic factor binding to its receptor is dependent on chloride concentration: A possible feedback-control mechanism in renal salt regulation. *Circ. Res.* **86**, 1135–1139 (2000).
59. H. Ogawa, Y. Qiu, C. M. Ogata, K. S. Misono, Crystal structure of hormone-bound atrial natriuretic peptide receptor extracellular domain: Rotation mechanism for transmembrane signal transduction. *J. Biol. Chem.* **279**, 28625–28631 (2004).
60. H. Ogawa, Y. Qiu, J. S. Philo, T. Arakawa, C. M. Ogata, K. S. Misono, Reversibly bound chloride in the atrial natriuretic peptide receptor hormone-binding domain: Possible allosteric regulation and a conserved structural motif for the chloride-binding site. *Protein Sci.* **19**, 544–557 (2010).
61. F. van den Akker, X. Zhang, M. Miyagi, X. Huo, K. S. Misono, V. C. Yee, Structure of the dimerized hormone-binding domain of a guanylyl-cyclase-coupled receptor. *Nature* **406**, 101–104 (2000).

62. C. M. Johannessen, J. S. Boehm, S. Y. Kim, S. R. Thomas, L. Wardwell, L. A. Johnson, C. M. Emery, N. Stransky, A. P. Cogdill, J. Barretina, G. Caponigro, H. Hieronymus, R. R. Murray, K. Salehi-Ashtiani, D. E. Hill, M. Vidal, J. J. Zhao, X. Yang, O. Alkan, S. Kim, J. L. Harris, C. J. Wilson, V. E. Myer, P. M. Finan, D. E. Root, T. M. Roberts, T. Golub, K. T. Flaherty, R. Dummer, B. L. Weber, W. R. Sellers, R. Schlegel, J. A. Wargo, W. C. Hahn, L. A. Garraway, COT drives resistance to RAF inhibition through MAP kinase pathway reactivation. *Nature* **468**, 968–972 (2010).
63. S. K. Mishra, S. Holzman, M. A. Hoon, A nociceptive signaling role for neuromedin B. *J. Neurosci.* **32**, 8686–8695 (2012).
64. N. T. Southall, A. Jadhav, R. Huang, Enabling the large-scale analysis of quantitative high-throughput screening data, in *Handbook of Drug Screening*, R. Seethala, L. Zhang, Eds. (Taylor and Francis, ed. 2, 2009), pp. 442–464.
65. A. Yasgar, P. Shinn, A. Jadhav, D. Auld, S. Michael, W. Zheng, C. P. Austin, J. Inglese, A. Simeonov, Compound management for quantitative high-throughput screening. *JALA* **13**, 79–89 (2008).
66. N. Thorne, M. Shen, W. A. Lea, A. Simeonov, S. Lovell, D. S. Auld, J. Inglese, Firefly luciferase in chemical biology: A compendium of inhibitors, mechanistic evaluation of chemotypes, and suggested use as a reporter. *Chem. Biol.* **19**, 1060–1072 (2012).
67. A. Avdeef, M. Strafford, E. Block, M. P. Balogh, W. Chambliss, I. Khan, Drug absorption in vitro model: Filter-immobilized artificial membranes. 2. Studies of the permeability properties of lactones in Piper methysticum Forst. *Eur. J. Pharm. Sci.* **14**, 271–280 (2001).
68. P. Shah, E. Kerns, D.-T. Nguyen, R. S. Obach, A. Q. Wang, A. Zakharov, J. McKew, A. Simeonov, C. E. C. A. Hop, X. Xu, An automated high-throughput metabolic stability assay using an integrated high-resolution accurate mass method and automated data analysis software. *Drug Metab. Dispos.* **44**, 1653–1661 (2016).
69. S. K. Mishra, S. M. Tisel, P. Orestes, S. K. Bhangoo, M. A. Hoon, TRPV1-lineage neurons are required for thermal sensation. *EMBO J.* **30**, 582–593 (2011).
70. B. J. Jones, D. J. Roberts, The quantitative measurement of motor inco-ordination in naive mice using an accelerating rotarod. *J. Pharm. Pharmacol.* **20**, 302–304 (1968).
71. S. M. Kim, C. Eisner, R. Faulhaber-Walter, D. Mizel, S. M. Wall, J. P. Briggs, J. Schnermann, Salt sensitivity of blood pressure in NKCC1-deficient mice. *Am. J. Physiol. Renal Physiol.* **295**, F1230–F1238 (2008).
72. Y. Kawashima, K. Kameo, M. Kato, M. Hasegawa, K. Tomisawa, K. Hatayama, S. Hirono, I. Moriguchi, Structure-activity studies of 3-benzoylpropionic acid derivatives suppressing adjuvant arthritis. *Chem. Pharm. Bull.* **40**, 774–777 (1992).

**Acknowledgments:** We thank C. Klumpp-Thomas for automated screening support; the NCGC compound management team for sample preparation; X. Xu, P. Shah, and A. Wang for PK studies; and R. MacArthur for informatics assistance. We thank A. Noguchi (NHLBI Phenotyping Core) for measuring cardiovascular studies and C. Xiao (NIDDK) for performing locomotor measurements. Human tissue was obtained from the NIH NeuroBioBank at the University of Maryland, Baltimore, MD. **Funding:** This work was supported by the intramural research program of the National Institute of Dental and Craniofacial Research, NIH, project ZIADE000721-18 (to M.A.H.), and the National Center for Advancing Translational Sciences, NIH, project 1ZIATR000053-04 (to J.I.). **Author contributions:** H.J.S., P.D., J.I., and M.A.H. designed the experiments. H.J.S., P.D., and E.O. performed the HTS. H.J.S., T.W.E., and X.G. were involved in the animal behavioral experiments. H.J.S., P.D., and J.B. analyzed HTS data, and H.J.S. analyzed all other data. H.J.S., P.D., J.I., and M.A.H. wrote and edited the paper, with comments from all authors. **Competing interests:** The NIH has a pending patent application (Compositions and methods for the inhibition of pruritus, no. 62/581,420) that covers part of the work described in this manuscript (H.J.S., P.D., J.I., and M.A.H.). **Data and materials availability:** All the data for this study are present in the main text or in the Supplementary Materials. In addition, pharmacological screening data have been deposited with PubChem (see table S8).

Submitted 26 September 2018
Resubmitted 19 February 2019
Accepted 30 May 2019
Published 10 July 2019
10.1126/scitranslmed.aav5464

**Citation:** H. J. Solinski, P. Dranchak, E. Oliphant, X. Gu, T. W. Earnest, J. Braisted, J. Inglese, M. A. Hoon, Inhibition of natriuretic peptide receptor 1 reduces itch in mice. *Sci. Transl. Med.* **11**, eaav5464 (2019).

Science Translational Medicine

# Inhibition of natriuretic peptide receptor 1 reduces itch in mice

Hans Jürgen Solinski, Patricia Dranchak, Erin Oliphant, Xinglong Gu, Thomas W. Earnest, John Braisted, James Inglese and Mark A. Hoon

*Sci Transl Med* **11**, eaav5464.
DOI: 10.1126/scitranslmed.aav5464

**Let him that itches block NPR1**

Chronic itch is an uncomfortable sensation with major impact on the quality of life. The pathophysiology of itch is not clearly elucidated, and the few available treatments are mostly ineffective. The natriuretic peptide receptor 1 (NPR1) has been recently shown to promote itch in mice; however, a peptide NPR1 inhibitor showed poor effects in mice. Investigating the reason for these negative results, Solinski *et al*. now show that the reported NPR1 inhibitor acted as partial agonist of the receptor, thus explaining the failure in relieving itch. Using high-throughput screening, the authors identified small-molecule human NPR1 antagonists. The molecules were able to relieve chronic itch in mice without inducing adverse effects.